Band structure of substoichiometric titanium nitrides and carbonitrides: spectroscopical and theoretical investigations

1997 J. Phys.: Condens. Matter 9 8453

(http://iopscience.iop.org/0953-8984/9/40/012)

J. Phys.: Condens. Matter **9** (1997) 8453–8463. Printed in the UK PII: S0953-8984(97)82380-6

Band structure of substoichiometric titanium nitrides and carbonitrides: spectroscopical and theoretical investigations

M Guemmaz†, G Moraitis‡, A Mosser†, M A Khan‡ and J C Parlebas‡

† GSI, IPCMS (UM 46 CNRS), 23 rue du Loess, 67037 Strasbourg Cédex, France

‡ GEMM, IPCMS (UM 46 CNRS), 23 rue du Loess, 67037 Strasbourg Cédex, France

Received 6 March 1997, in final form 30 June 1997

Abstract. Recently, substoichiometric titanium nitrides TiN_x ($x = 0.45$ and 0.61) and carbonitrides TiC_xN_y ($x = y = 0.35$) have been synthesized by multiple-energy ion implantation at the surface of pure titanium. Changes in the binary and ternary alloy electronic properties versus defect impurity and vacancy concentrations have been studied by means of core Ti 2p and valence x-ray photoemission spectra (XPS). Moreover, self-consistent tight-binding linear-muffin-tin-orbital calculations with empty spheres in place of the missing nitrogen and/or carbon atoms give, among other information, the total density of occupied states, for comparison with the observed valence XPS value.

1. Introduction

It is well known that titanium carbides, nitrides and carbonitrides exhibit rather exceptional physical properties. Their electrical and thermal conductivities are close to those of pure metals. Their melting points allow one to consider them as refractory metals. The chemical stability at room temperature and the corrosion resistance of these compounds are very high, and the corresponding hardness is among the highest, after that of diamond [1, 2]. However, it is virtually impossible to produce these refractory compounds as single phases with their nominal formulae.

The electronic structure of the corresponding stoichiometric and near-stoichiometric metal compounds has been studied by many authors for quite a long time (see, e.g., [3, 4]) for the following two reasons. The first one is related to the synthesis methods which allow us to prepare these compounds very easily near the stoichiometry. The second one is the fact that the properties of these materials have been believed, thus far, to be at their most interesting near stoichiometry. Hence, much more is known about the properties of these stoichiometric and near-stoichiometric binary materials than is known about them far from stoichiometry. In particular, the low-nitrogen-concentration limits of the TiN_x compounds as well as the carbonitrides TiC_xN_y have not yet been studied systematically as far as we know.

In the present work, using multiple-energy (180, 100, 50, and 20 keV) ion implantation at a surface of titanium, substoichiometric titanium nitrides TiN_x ($x = 0.45$ and 0.61) and carbonitrides TiC_xN_y ($x = y = 0.35$) have been synthesized. For other concentrations, we refer the reader to [20]. Several techniques were used in order to characterize the layers thus synthesized [5–8]. All of the corresponding physical properties are related to their electronic structures. In this paper just our valence x-ray photoemission spectra (v-XPS) for Ti carbides, nitrides and carbonitrides are compared to the corresponding total

0953-8984/97/408453+11$19.50

densities of states (DOS) which we are able to analyse theoretically. Actually, the detailed interpretations of Ti 2p XPS spectra (see for example [8]) and especially the Ti 2p satellite structure [9] are outside the scope of the present work and will be presented elsewhere. However, in this paper our v-XPS data for Ti nitrides and carbonitrides are compared to the corresponding total DOS. The calculations presented here for the electronic structure in the case of stoichiometric (and non-stoichiometric) TiN_x and TiC_xN_y compounds are performed within a self-consistent tight-binding linear-muffin-tin-orbital (TB-LMTO) method.

For stoichiometric TiN and non-stoichiometric TiN_x compounds, there are many v-XPS results available in the literature [9–13]. For stoichiometric TiN compounds, the peak positions and widths agree fairly well with band-structure calculations [10, 11], whereas for substoichiometric TiN_x some discrepancies were found [12] between the experimental and theoretical results [14]. Let us emphasize that the v-XPS spectra of TiN_x have already been measured over the entire composition range of the rock-salt structure (with $0.5 \leqslant x \leqslant 1$) and analysed in relation to various theoretical results [9]. The great difficulty in theoretical calculations of the electronic structure of non-stoichiometric materials is mainly due to the problem of taking proper account of the lattice vacancies. To treat the vacancy problem, some appropriate approximations have been made. Klima [14] has used a coherent-potential approximation (CPA) within a linear-combination-of-atomic-orbitals basis to calculate the total DOS of TiN_x (with $0.6 \leqslant x \leqslant 1$). The CPA was also applied to TiC_x and TiN_x compounds by Marksteiner *et al* [15] but within a Korringa–Kohn–Rostoker method. Besides this completely disordered version, there have been a number of self-consistent band-structure calculations for the TiN_x systems near the stoichiometric limit, without [16] or with [17] local lattice relaxation. Recently, using a TB-LMTO method [18, 19] with ordered empty spheres for the vacancies, we were able to analyse the experimental v-XPS spectra for various concentrations of TiC_x obtained from ion implantation [20]. Here, we extend this work to TiN_x and TiC_xN_y compounds and compare the results with our recent v-XPS data. Our calculations again introduce empty spheres, if necessary, in place of the missing nitrogen or/and carbon atoms.

The paper is organized as follows. In section 2 we present our experimental data for TiN_x and TiC_xN_y compounds with a special emphasis on v-XPS spectra. Next (section 3) we give the results of our electronic structure calculations for a series of Ti nitrides and carbonitrides. Section 4 is devoted to a discussion and conclusions.

2. Experimental study of TiN_x and TiC_xN_y: XPS results

Among the techniques that allow the synthesizing of titanium nitrides and carbonitrides, ion implantation is particularly attractive, since it provides a wide range of non-stoichiometric materials. Also, the coatings obtained by implantation have no abrupt interface, which prevents there from being problems of adherence with the substrate. Rectangular samples (10×15 mm^2) were cut from a titanium sheet, then polished mechanically, first with carborundum, then with diamond paste down to 0.25 μm. Afterwards the samples were washed with ethanol in an ultrasonic bath.

Multiple-energy ion implantation was performed with an EATON 200 MC implanter, equipped with a magnetic mass analyser. An electrostatic scanning system allowed delivery of a uniform dose over the whole sample surface. The vacuum during implantation was 10^{-6} Torr. The power dissipated in the samples during implantation was of the order of 100 mW cm^{-2}. Thus, since the samples were not cooled, their temperature reached 300 °C during implantation. With successive nitrogen and carbon implantations at several energies (180, 100, 50 and 20 keV), non-stoichiometric titanium nitrides TiN_x (with $x = 0.45$ and

0.61) and carbonitrides TiC_xN_y ($x = y = 0.35$) were prepared. The thickness of the layers was about 400 nm. The implanted atomic concentrations and profiles were measured respectively by Rutherford back-scattering (RBS) (the incident particles were 2 MeV $^4He^+$ ions concentrated in a beam of 2 mm diameter, and the back-scattering angle was 136°) and by secondary-ion mass spectrometry (SIMS) (the profiles were determined by dynamical SIMS with 10 keV argon ions and an incident beam diameter of 0.1 mm) [7]. The samples present profiles which indicate that the concentration is approximately uniform over the whole implanted range. This was also confirmed by the corresponding SIMS spectra. The crystallographic structure of the layers was determined by grazing-incidence x-ray diffraction.

The XPS analysis was performed with a VG II apparatus equipped with two chambers: a preparation chamber where the 5 keV argon-ion etches were performed with a cold-cathode ion gun and an analyser chamber where the photoelectrons excited by the Al Kα radiation were analysed with a hemispherical analyser. Let us just be precise that the argon sputtering of the samples (to remove the contamination) was performed under grazing incidence in order to minimize argon embedding and creation of extra vacancies. On the other hand, one should notice that the extra vacancies introduced by SIMS and RBS measurements are negligible compared to those due to the substoichiometry. The analyser pass energy was fixed at 20 eV, which corresponds to about 0.6 eV resolution. Taking into account the Al K$\alpha_{1,2}$ linewidth, the whole apparatus resolution was about 1.2 eV. The energy calibration was realized by setting the Au $4f_{7/2}$, the Cu L_3VV, and the Cu $2p_{3/2}$ peaks at energies equal to, respectively, 84.0, 568.0, and 932.7 eV. The vacuum was maintained at 10^{-10} Torr during the measurements with a cryopumping system.

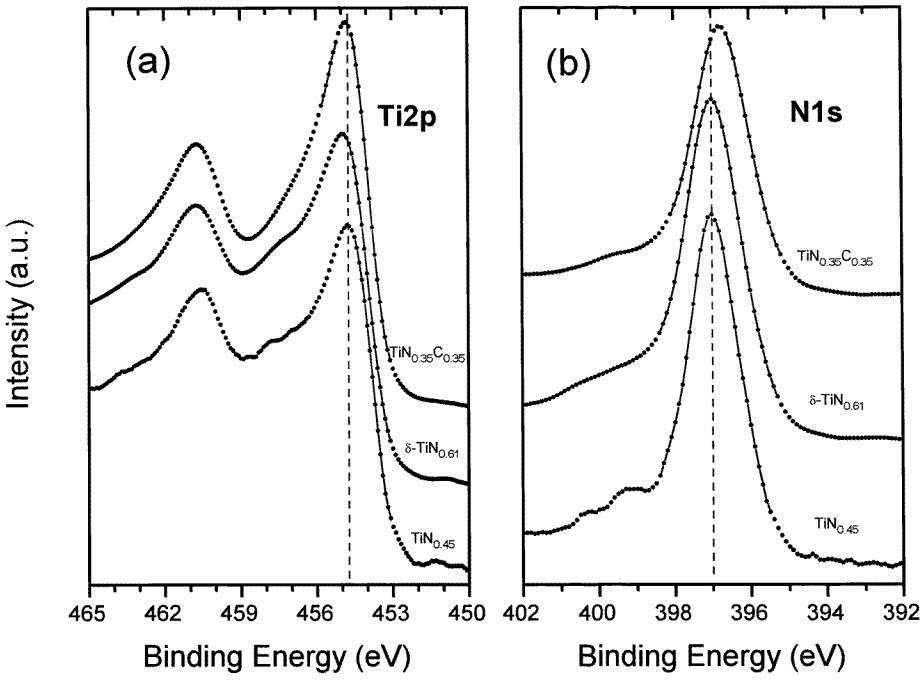

Figure 1. Experimental Ti 2p (a) and N 1s (b) XPS spectra of the compounds $TiC_{0.35}N_{0.35}$, δ-$TiN_{0.61}$, and $TiN_{0.45}$.

The XPS spectra showed that the surfaces of several samples were mainly covered with titanium oxide (probably TiO_2) which disappears quickly under argon bombardment. In order to reduce the selective sputtering effect due to argon bombardment on the surface composition, this cleaning procedure was carried out for a small angle of incidence. Thus, we believe that the argon bombardment did not extensively affect the recorded spectra.

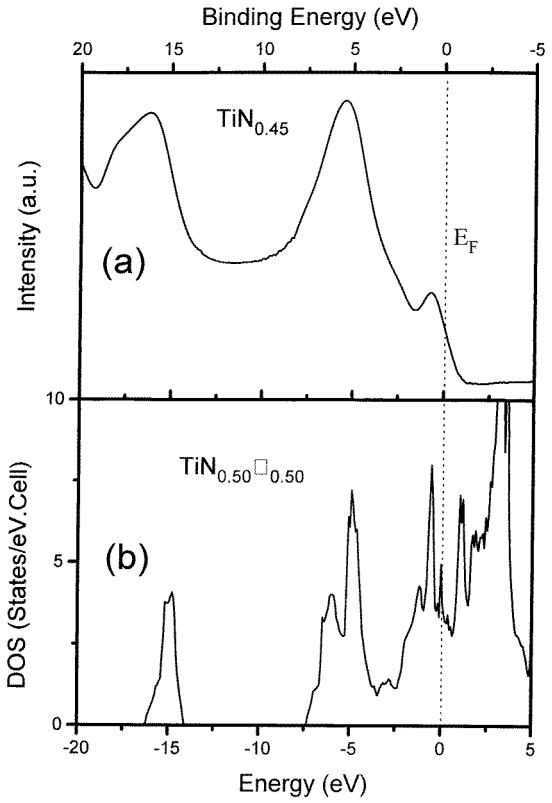

Figure 2. The experimental v-XPS spectrum of $TiN_{0.45}$ (a) compared to the calculated $TiN_{0.50}\square_{0.50}$ total DOS (b).

Figure 1 shows the Ti 2p and the N 1s photoelectron lines corresponding to the two titanium nitrides, $TiN_{0.45}$ and $TiN_{0.61}$, and the titanium carbonitride. The N 1s photoelectron peak positions of titanium nitride reported in the literature vary from 396.3 to 397.7 eV, depending on the preparation method, on treatments undergone by the samples and on the accuracy of the analyser calibration. One can notice that the position of the N 1s peak corresponding to the two nitrides is remarkably constant at 397.0 eV (figure 1(b)). The width (1.5 eV) at half-maximum of the corresponding two peaks is also constant, and this value is in good agreement with those given by Pivin *et al* [21] and Bertoncello *et al* [22]. No energy change was observed for the N 1s peak corresponding to nitrogen in solid solution and nitrogen in the δ-$TiN_{0.61}$ phase, even if the chemical neighbourhood of the nitrogen atoms is different in the two structures. We believe that the energy displacement involved in such a structural change is not big enough to be visible with usual apparatus. In the $TiN_{0.35}C_{0.35}$ case, the N 1s peak appears at 396.7 eV, a position slightly different from that for the nitrides. We do not show the C 1s level, but it actually appears as two

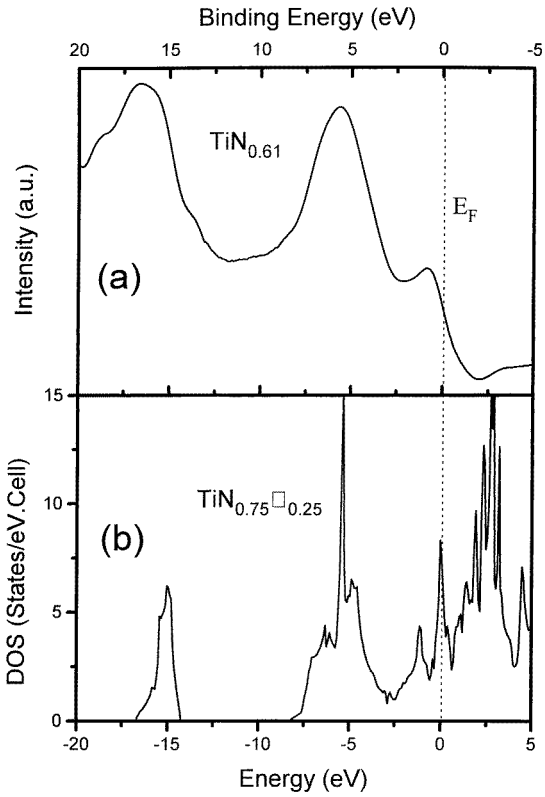

Figure 3. The experimental v-XPS spectrum of $TiN_{0.61}$ (a) compared to the calculated $TiN_{0.75}\square_{0.25}$ total DOS (b) (for technical reasons, the ordinate scale of figure 3(b) is different from those of figures 2(b) and 4(b)).

peaks. The one at 284.6 eV is associated with the formation of graphite at the surface of the sample which remains present even after a long-duration argon-ion bombardment; the other at 281.6 eV is characteristic of the carbonitride. It is interesting to notice that the C 1s peak of the titanium carbides appears also at 281.6 eV [23]. It is worth mentioning the absence of a comparable graphite peak in our nitride spectra recorded under the same conditions. Therefore, the origin of this peak cannot be related to the titanium substrate preparation using diamond polishing. The shapes of the nitride Ti $2p_{3/2}$ and Ti $2p_{1/2}$ peaks are complex, as several authors have reported [24, 25], and one can see (figure 1(a)) that they contain at least two contributions: the first due to titanium nitride and the second associated with titanium oxide (not necessarily TiO_2) located at the surface as a consequence of the gettering of the residual oxygen.

In their studies on titanium nitrides, Porte *et al* [9] report in Ti 2p transitions the existence of a strong line at 2.2 eV higher binding energy for compositions near stoichiometry ($x > 0.8$). This is probably related to the decreased screening effect of the conduction electrons. On the other hand, Vasile *et al* [26] have shown that the Ti 2p peak shape is a function of the nitrogen concentration, and that oxygen contributes significantly to the background formation. In a study of the titanium nitride energy losses, Strydom and Hofmann [25] pointed out that the losses due to intraband transitions change the shape of the Ti 2p transitions. These different phenomena make it difficult to interpret the titanium

nitride and carbonitride XPS spectra quantitatively. In other respects, one may notice that the Ti 2p peak is shifted progressively towards higher binding energies as a function of increasing nitrogen concentration due to the charge transfer from Ti atoms to N atoms, which indicates an ionic contribution in the Ti–N bonding.

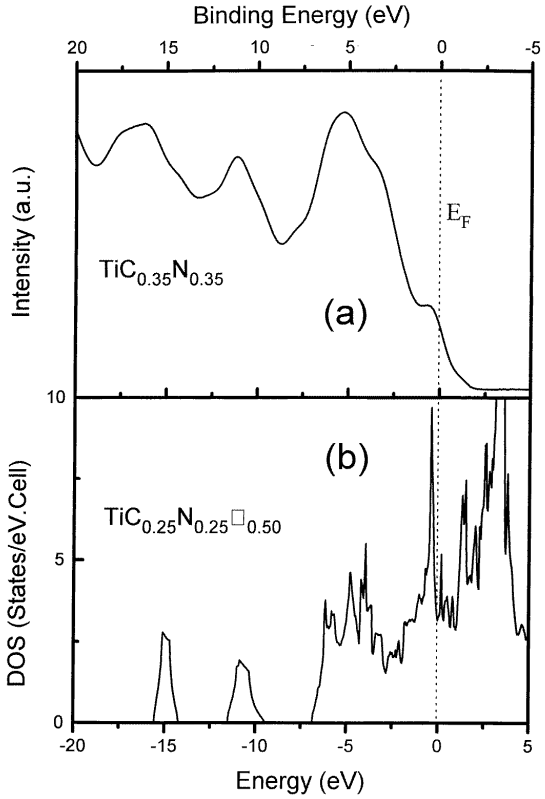

Figure 4. The experimental v-XPS spectrum of $TiC_{0.35}N_{0.35}$ (a) compared to the calculated $TiC_{0.25}N_{0.25}\square_{0.50}$ total DOS (b).

In order to compare our experimental results to the theory (see section 3), the nitride valence band spectra are shown in figures 2(a) and 3(a) which display three characteristic structures:

(i) a peak at about 16.5 eV binding energy, corresponding to the N 2s electron band;

(ii) a strong peak at 5.5 eV due to the Ti 3d–N 2p hybridization which gives a covalent character to the Ti–N binding and determines the high stability of the titanium nitrides; and

(iii) a shoulder near the Fermi level.

These three characteristic structures have already been observed for an angle-integrated photoemission spectrum recorded from $TiN_{0.83}$ substoichiometric compounds [1]; in particular the feature just below the Fermi level is present. Also, similar phenomena are observed in the valence band of the titanium carbonitride with an additional peak associated with the C 2s electron band at about 11 eV binding energy (figure 4(a)).

Table 1. The lattice parameter and density of states at the Fermi level for several stoichiometric compounds.

	$TiN_{1.00}$	$TiC_{0.25}N_{0.75}$	$TiC_{0.50}N_{0.50}$	$TiC_{0.75}N_{0.25}$	$TiC_{1.00}$
Lattice parameter (nm)	0.4241	0.4263	0.4284	0.4306	0.4327
$n(E_F)$ (states Ryd^{-1})	2.98	2.64	2.25	1.76	1.66

Table 2. The lattice parameter and density of states at the Fermi level for several substoichiometric compounds with 25% vacancies.

	$TiN_{0.75}\square_{0.25}$	$TiC_{0.25}N_{0.50}\square_{0.25}$	$TiC_{0.50}N_{0.25}\square_{0.25}$	$TiC_{0.75}\square_{0.25}$
Lattice parameter (nm)	0.4228	0.4256	0.4285	0.4315
$n(E_F)$ (states Ryd^{-1})	7.92	4.61	2.94	2.86

Table 3. The lattice parameter and density of states at the Fermi level for several substoichiometric compounds with 50% vacancies.

	$TiN_{0.50}\square_{0.50}$	$TiC_{0.25}N_{0.25}\square_{0.50}$	$TiC_{0.50}\square_{0.50}$
Lattice parameter (nm)	0.4215	0.4258	0.4301
$n(E_F)$ (states Ryd^{-1})	4.53	5.16	14.51

3. Electronic structure calculation of Ti nitrides and carbonitrides

For simplicity our calculations are restricted to the NaCl crystallographic structure whereas $TiN_{0.25}$ is hexagonal and $TiN_{0.45}$ is a mixture of hexagonal and NaCl structures. Nevertheless, a NaCl band-structure calculation of TiN_x for the whole range of concentration already gives important information that can be compared to the v-XPS data. The same remark holds for TiC_xN_y. The NaCl lattice is composed of two face-centred cubic (fcc) sublattices, one containing the titanium atoms and the other the metalloid atoms (C or/and N). For the electronic structure calculation we use the TB-LMTO method [18, 19]: the exchange–correlation effect is included through the local density approximation (LDA). For a discussion of this last approximation, we refer the reader to Ahuja *et al* [27]. For Ti, we consider s, p, d orbitals corresponding to four valence electrons ($3d^24s^24p^0$); for C we have $2s^22p^2$ electrons and for N we have $2s^22p^3$ electrons. The departure from stoichiometry in $TiN_x\square_{1-x}$ ($0 < x < 1$) and $TiC_xN_y\square_{1-x-y}$ ($0 < x + y < 1$) is described by ordered vacancies (□) with empty Wigner–Seitz spheres in the metalloid lattice. The configurations Ti_4N_4, $Ti_4N_3\square_1$, $Ti_4N_2\square_2$, and $Ti_4N_1\square_3$ correspond respectively to $x = 1$, 0.75, 0.5, and 0.25, and an increasing concentration $(1-x)$ of vacancies. The stoichiometric carbonitrides,

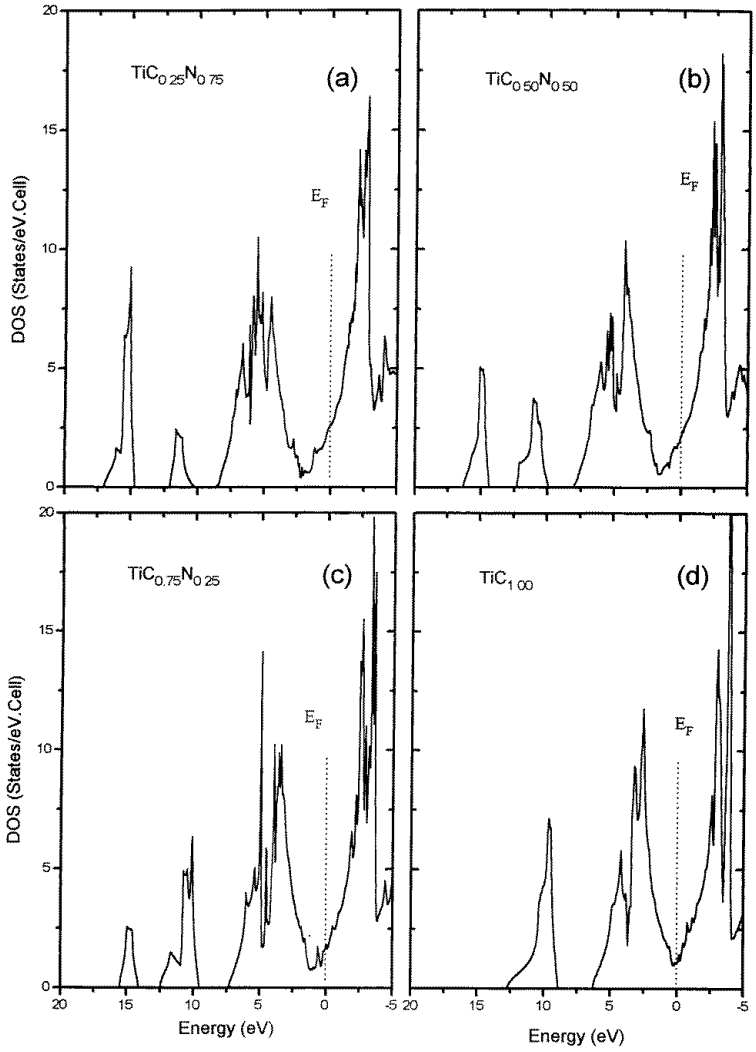

Figure 5. The theoretical total DOS of stoichiometric $TiC_xN_{(1-x)}$ for: (a) $x = 0.25$; (b) $x = 0.50$; (c) $x = 0.75$; and (d) $x = 1.00$.

$Ti_4C_1N_3$, $Ti_4C_2N_2$, and $Ti_4C_3N_1$ correspond to TiC_xN_y with $(x, y) = (0.25, 0.75)$, (0.50, 0.50), and (0.75, 0.25). It is obvious that the lattice parameter of titanium carbonitrides is a function of their composition. Thus, for stoichiometric TiC_xN_{1-x} carbonitrides it varies linearly from $a = 0.4241$ nm for TiN to $a = 0.4327$ nm for TiC (table 1).

Finally, the substoichiometric carbonitrides $Ti_4C_2N_1\square_1$, $Ti_4C_1N_2\square_1$, and $Ti_4C_1N_1\square_2$ correspond to $TiC_xN_y\square_z$ with, respectively, $(x, y, z) = (0.50, 0.25, 0.25)$, (0.25, 0.50, 0.25), and (0.25, 0.25, 0.50). Tables 2 and 3 respectively give the linear interpolation for the lattice parameter in the case of one or two vacancies per unit cell. For the k-space integration by the tetrahedron method, 405 k-points are used in the irreducible Brillouin zone. This number of k-points is found to be sufficient for obtaining a completely converged result. Also, all of the electronic energies are given with reference to the Fermi energy E_F.

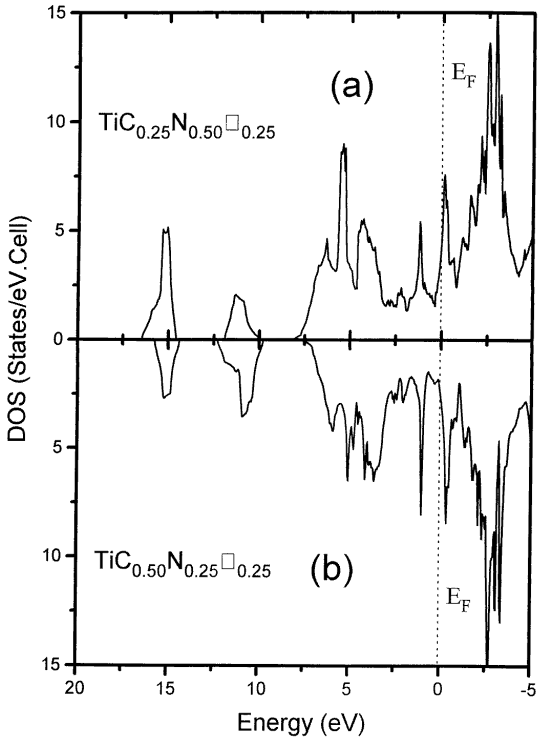

Figure 6. The theoretical total DOS of substoichiometric $TiC_xN_y\square_{(1-x-y)}$ for: (a) $x = 0.25$, $y = 0.50$; and (b) $x = 0.50$, $y = 0.25$.

Figure 2(b) and figure 3(b) report the calculated DOS of TiN_x for $x = 0.50$ and 0.75. As is well known, TiN is qualitatively similar to TiC [20], except that E_F now falls above the pseudogap minimum because of the additional 2p nitrogen electron. Therefore, $n(E_F)$ is increased when going from TiC to TiN. This effect is even more pronounced when going from $TiC_{0.75}$ to $TiN_{0.75}$ [20], since in the nitrides, 'vacancy states' appear as a superstructure right at E_F (figure 3(b)). The inverse situation is found between $TiC_{0.50}$ and $TiN_{0.50}$. Of course we can check in figures 3(b) and 2(b) that the intensity of the filled N 2s peak is decreasing with decreasing N concentration.

The total DOS of the stoichiometric carbonitrides TiC_xN_y is shown in figures 5(a), 5(b), 5(c), and 5(d) for $(x, y) = (0.25, 0.75)$, (0.50, 0.50), (0.75, 0.25), and (1, 0) respectively. The first two peaks on the left-hand side originate from N 2s and C 2s, and their intensities are proportional to y and x respectively. Let us also remark that in the evolution from TiN to TiC (cf. figure 5(d) and table 1) a progressive shift of the Fermi level to the minimum of the density of states can be noticed.

Finally, figures 6(a), 6(b) and 4(b) report our calculated DOS for the substoichiometric carbonitrides $TiC_xN_y\square_z$, with (x, y, z) being, respectively, (0.25, 0.50, 0.25), (0.50, 0.25, 0.25), and (0.25, 0.25, 0.50). Tables 2 and 3 show the corresponding interpolated lattice parameters. Again we distinguish the N 2s and C 2s peaks on the left-hand side of the energy scale. Also, vacancy states are visible as superstructures in all three figures, but only $TiC_{0.25}N_{0.50}\square_{0.25}$ (figure 6(a)) presents a peak of the DOS at the Fermi level.

4. Discussion and concluding remarks

In order to facilitate the comparison between theory and the experimental spectra we have shown our calculated DOS for $TiN_{0.50}$ and $TiN_{0.75}$ (figures 2(b) and 3(b)) just below the measured v-XPS of $TiN_{0.45}$ and $TiN_{0.61}$ (figure 2(a) and figure 3(a)). Let us first comment that the theoretical DOS that we choose to show in figures 2 to 4 are the true TB-LMTO DOS without any treatment to incorporate experimental contingencies. However, in order to make somewhat clearer the comparison of theory with experiment (figure 2(a), for example), we have to bear two things in mind:

(i) there is a well known background addition which should be removed to facilitate comparison with the DOS; and

(ii) the experimental spectra cannot display as many details as the theoretical DOS due to a broadening factor which reflects the experimental energy resolution.

Of course a Gaussian or Lorentzian convolution of the theoretical DOS (see reference [8] and references therein) will certainly bring it closer to the experimental data, i.e. essentially a smooth Fermi edge peak as well as a broad 5 eV valence band bump. Nevertheless, these features already come out directly from our TB-LMTO calculations. Although the stoichiometries do not exactly coincide, the small peak at about 1 eV below E_F exists both experimentally and theoretically, as well as the one at around 5.5 eV below E_F. There is a slight difference in the energy position when looking at the N 2s peak; however, the overall agreement is quite satisfactory. The same agreement can be observed in figure 4, where we compare our theoretical DOS for $TiC_{0.25}N_{0.25}$ to the v-XPS spectrum of $TiC_{0.35}N_{0.35}$, although here also the stoichiometries are slightly different.

As a conclusion, we can say that we have been quite successful in studying the interesting effect of atoms (C, N) and vacancy concentrations on the electronic structure of (sub)stoichiometric TiN_x and TiC_xN_y compounds. The existence of vacancy (superstructure) states in the TiN and TiCN pseudogaps is confirmed both by our v-XPS measurements and by our *ab initio* calculations.

References

[1] Johansson L I 1995 *Surf. Sci. Rep.* **21** 177
[2] Ohring M 1992 *The Materials Science of Thin Films* (San Diego, CA: Academic)
[3] Neckel A 1990 *The Physics and Chemistry of Carbides* ed R Freer (Dordrecht: Kluwer Academic) pp 485–511
[4] Skala L and Capkova P 1990 *J. Phys.: Condens. Matter* **2** 8293
[5] Guemmaz M, Mosser A, Raiser D, Grob J J, Cornet A and Paletto S 1995 *Mater. Res. Soc. Symp. Proc.* **354** 243
[6] Guemmaz M, Mosser A, Grob J J, Sens J C and Stuck R 1996 *Surf. Coatings Technol.* **80** 53
[7] Guemmaz M, Mosser A and Grob J J 1997 *Appl. Phys.* A **64** 407
[8] Parlebas J C, Khan M A, Uozumi T, Okada K and Kotani A 1995 *J. Electron Spectrosc. Relat. Phenom.* **71** 117
[9] Porte L, Roux L and Hanus J 1983 *Phys. Rev.* B **28** 3214
[10] Johansson L I, Stefan P M, Shek M L and Christensen A N 1980 *Phys. Rev.* B **22** 1032
[11] Neckel A 1983 *Int. J. Quantum Chem.* **23** 1317
[12] Höchst H, Bringans R D, Steiner P and Wolf T 1982 *Phys. Rev.* B **25** 7183
[13] Kutznetsov M V, Zhuralev J F, Zhilyaev V A and Gubanov V A 1992 *J. Electron Spectrosc. Relat. Phenom.* **58** 1
[14] Klima J 1979 *J. Phys. C: Solid State Phys.* **12** 3691
Klima J 1980 *Czech J. Phys.* B **30** 905
[15] Marksteiner P, Weinberger P, Neckel A, Zeller R and Dederichs P H 1986 *Phys. Rev.* B **33** 812

[16] Ivanovsky A L, Anisimov V I, Novikov D L, Lichtenstein A I and Gubanov V A 1988 *J. Phys. Chem. Solids* **94** 465
[17] Capkova P and Skala L 1992 *Phys. Status Solidi* b **171** 85
[18] Andersen O K and Jepsen O 1984 *Phys. Rev. Lett.* **53** 2571
[19] Andersen O K, Pawlowska Z and Jepsen O 1986 *Phys. Rev.* B **34** 5253
[20] Guemmaz M, Moraitis G, Mosser A, Khan M A and Parlebas J C 1997 *J. Electron Spectrosc. Relat. Phenom.* **83** 173
[21] Pivin J C, Pons F, Takadoum J, Pollock H M and Farges J 1987 *J. Mater. Sci.* **22** 1087
[22] Bertoncello R, Casagrande A, Casarin M, Glisenti A, Lanzoni E, Mirenghi L and Tondello E 1992 *Surf. Interface Anal.* **18** 525
[23] Guemmaz M, Mosser A, Boudoukha L, Grob J J, Raiser D and Sens J C 1996 *Nucl. Instrum. Methods* B **111** 263
[24] Hofmann S 1986 *J. Vac. Sci. Technol.* A **4** 2789
[25] Strydom I leR and Hofmann S 1991 *J. Electron Spectrosc. Relat. Phenom.* **56** 85
[26] Vasile M J, Emerson A B and Baiocchi F A 1990 *J. Vac. Sci. Technol.* A **8** 99
[27] Ahuja R, Ericksson O, Wills J M and Johansson B 1996 *Phys. Rev.* B **53** 3072